

Determination of Biomass Power Plant Location Using GIS-Based Heuristic Methods: A Case Study in Turkey

Adem AKGÜL

Gaziantep University: Gaziantep Universitesi

Serap Seçkiner (✉ seckiner@gantep.edu.tr)

Gaziantep University: Gaziantep Universitesi <https://orcid.org/0000-0002-1612-6033>

Research Article

Keywords: Biomass Energy, Supply Chain Optimization, Facility Location Problem, Tri-generation, Simulated Annealing

Posted Date: January 14th, 2022

DOI: <https://doi.org/10.21203/rs.3.rs-953284/v1>

License:   This work is licensed under a Creative Commons Attribution 4.0 International License.

[Read Full License](#)

1 **Determination of biomass power plant location using GIS based heuristic methods: A case**
2 **study in Turkey**

3 Adem AKGÜL, Serap ULUSAM SEÇKİNER*

4 Department of Industrial Engineering, Gaziantep University, 27310, Gaziantep/TURKEY

5
6 **Abstract**

7 Biomass conversion to bioenergy has always been necessary to ensure the most efficient use of
8 the limited biomass resource and enable economic viability. Evaluating biomass transportation
9 cost, electricity transmission cost and heat transferring cost between power plant location/s and
10 supply/demand points and selection of an optimum power plant capacity is an important issue for
11 a robust supply chain design. In this study, we employed designing optimum biomass to the
12 bioenergy supply chain for agricultural activities using Geographic Information System and
13 Simulated Annealing algorithm to overcome a real-world problem in Bismil District of
14 Diyarbakır/Turkey. Our goal is to define a potential investment location/s on the trigeneration
15 system by comparing the trade-offs between the raw material/end-product transportation costs
16 and facility/s and pipeline installation costs. To determine possible locations for power plants,
17 distance matrices were retrieved from suitable candidate power plant locations and agricultural
18 parcel, settlement and the nearest high voltage electricity line from the Geographic Information
19 System. The results showed that establishing one power plant is feasible. The net present value
20 of a potential investment is almost 260 million Euros and the re-payment period is 1.33 years.

21 **Keywords:** Biomass Energy, Supply Chain Optimization, Facility Location Problem, Tri-
22 generation, Simulated Annealing.

23
24
25
26
27
28

*Corresponding author
E-mail addresses: seckiner@gantep.edu.tr (S.Seçkiner)

29 **1. Introduction**

30 Biomass can be defined as the total mass of living organisms that belong to a society consists of
31 species or consist of several species. Biomass is the most widely used renewable energy source
32 in the world today. It is contributing to energy used in power generation, generating electricity,
33 heating homes, fueling vehicles, heat for industry and buildings, and transport (IEA 2017).
34 Today, the key notion in biomass utilization is excluding the traditional use of biomass. Biomass
35 is commonly converted to energy through traditional methods that lead to inefficiency, health
36 problems, and environmental pollution (Akgül and Seçkiner 2019). Efficiency varies from 5% to
37 15% in traditional methods; however, it reaches up to 90% in modern bioenergy facilities.
38 Modern bioenergy term is generally used to refer to heat or electricity or transport biofuels and
39 exclude the traditional use of biomass.

40 According to a report published by International Energy Agency (IEA 2017), Global biofuel
41 production increased 10 billion liters in 2018 to reach a record 154 billion liters. Double
42 the growth of 2017, this 7% year-on-year increase was the highest in five years. Output is
43 forecast to increase 25% to 2024, an upwards revision from 2018 owing to better market
44 prospects in Brazil, the United States and especially China. The goal for the year 2060 is
45 17%. Modern and traditional biomass accounts for 70% of all renewable energy production and
46 nearly equivalent to that of coal in terms of final energy consumption. Electricity generated in
47 bioenergy power plants accounts for 2% of the total electricity production and % 8 of renewable
48 resource-based electricity production in the world in 2016. It is projected that biomass
49 utilization will contribute to providing 20% carbon saving up to 2060. The total biomass energy
50 potential of Turkey is about 33 million tons of oil equivalents (Mtoe). The amount of usable
51 biomass potential of Turkey is approximately 17 Mtoe. The electrical production potential from
52 usable bioenergy sources is 73 MW in 2010 and corporate income and represents more than
53 280,000 jobs (Toklu 2017). The traditional use of biomass is undesirable for both economic and
54 environmental reasons. Governments across the world encourage the private sector to produce
55 electricity from renewable energy resources. Turkey is one of these states, which has incentive
56 tools with regards to renewable resource utilization. According to renewable energy law enacted
57 in 2005, electricity generation from biomass and solar power has the highest price (13.3 USD
58 Cent/kWh) guaranteed by the government. That price can reach up 18,1 USD Cent/kWh in case
59 of utilizing national machines or equipment in power plants. However, the price of electricity
60 generated from wind and geothermal power are 7.3 and 10.5 USD Cent/kWh, respectively. This
61 indicates that energy production from biomass is the most valuable compared to other renewable
62 energy resources.

63 Bioenergy accounts for 1.5% of renewable-based electricity production including hydropower in
64 Turkey. This share is 0.7% when considering all kinds of electricity generation (General
65 Directorate of Energy Affairs 2018). As might be seen from the figures, Turkey is below the
66 world average in terms of bioenergy utilization. Given the limited natural energy reserves and
67 extensiveness of agricultural lands of the country, the share of bioenergy is relatively low. The
68 government has noticed this situation and set the goals to increase biomass utilization in modern
69 conversion plants. Installed power of 1000 MW is targeted in biomass-based electricity
70 generation in National Renewable Energy Action Plan. Biomass exploitation has crucial
71 importance to reach this goal.

72 Biomass exploitation in modern conversion plants has increased in recent years. What drives this
73 improvement are summarized as follows:

- 74 • Biomass can secure access to reliable energy resources,
- 75 • Carbon-neutrality is one of the major advantages of biomass energy
- 76 • Biomass utilization can make possible to earn more income for people living in rural areas,
- 77 • Bioenergy can be stored in liquid and gas form as an end or by-product,
- 78 • Biomass is a sustainable energy resource unlike fossil fuels
- 79 • Generating energy from biomass materials can greatly help in waste management
- 80 • Biomass energy is estimated to have a huge potential due to the abundant availability of
81 biomass sources

82 Apart from the advantages, there are still some disadvantages to biomass exploitation in modern
83 energy conversion plants. They are summarized as follows:

- 84 • Biomass contains carbon and it releases carbon dioxide on combustion and the time to
85 recapture the carbon involved in biomass may vary depending on the type of biomass.
- 86 • Uncertainties in quantity,
- 87 • Unavailability in a given period (seasonal fluctuation),
- 88 • The construction and operating costs of a biomass energy plant can be expensive concerning
89 traditional forms of power generation.
- 90 • Storage facilities require huge space, as harnessing energy from biomass involves a selection
91 of different processes.
- 92 • High collection cost due to its geographically scattered structure,

93 Governments have some incentive tools to increase biomass utilization in modern facilities.
94 Decrease of external dependence in energy supply and carbon emission is targeted thanks to

95 these incentives by governments. The high unit installation cost of bioenergy facility compared
96 to fossil fuel-based facility is compensated with these subventions. Despite the incentives,
97 biomass' geographically scattered structure, high transportation cost, seasonal fluctuation and
98 uncertainty in quantity may make a potential investment infeasible at first glance. The collection
99 and transportation cost of biomass accounts for 33-50% of the total biomass-to-bioenergy supply
100 chain cost (Kumar et al. 2006) Drawbacks in the biomass-to-bioenergy supply chain can be
101 eliminated through the scientific approach. Spatial analysis tools and optimization technics are
102 convenient methods for designing a robust energy supply chain.

103 The remainder of this paper is organized as follows. Section 2 presents a literature review about
104 other works closely related to the biomass to bio-energy supply chain problems which are solved
105 through meta-heuristic methods. In section 3, heuristic method, problem description and
106 geographic information system and spatial analysis tools for the problem dealt with are presented
107 in materials and methods section. The real-world problem is addressed in Section 4 to illustrate
108 the performance of the proposed heuristic technic. Finally, we conclude the paper and indicate
109 future research directions in Section 5.

110

111 **2. Literature review on biomass-to-bioenergy supply chain management**

112

113 Bioenergy is derived from biomass which is a carbon-based biological material. Biomass is
114 converted into energy via three main methods (Turkenburg 2000). Thermochemical, biochemical
115 and extraction. Biochemical conversion is generally suitable for biomass which has a moisture
116 content higher than 60% like livestock residues and wastewaters, while thermochemical methods
117 are suitable for the biomass whose organic dry matter is higher than 60% like lignocellulosic
118 material (Ciria et al. 2016). Lignocellulosic biomass, which is mainly composed of celluloses
119 and lignin, is mostly derived from agricultural and forest activities. Corn and cotton are
120 considered as a raw material in this study are an instance of lignocellulosic biomass.

121 Gasification, which is a thermochemical method, is considered as the biomass to gas conversion
122 process since it is a suitable technology for lignocellulosic biomass. At the end of this process,
123 syngas is produced which has a high calorific value and mainly composed of hydrogen, carbon
124 monoxide, water, and fewer undesired contaminants. The syngas can run through gas turbines or
125 other power conversion technology (prime mover) to produce electricity. Integrating some
126 auxiliary equipment to prime mover allows generating cooling, heating, and power
127 simultaneously. This is called trigeneration (combined cooling, heating, and power (CCHP)). In
128 a trigeneration system, total system efficiency can reach up to 85% at full load, almost 40% of

129 which is accounted for electric efficiency, remaining is the thermal efficiency (Akgül and
130 Seçkiner 2019). The load level affects the efficiency of prime mover positively. The district
131 heating and cooling system (DHCS) must be integrated into a trigeneration system to transfer hot
132 and cold heat demand points. Some parameters including pipe diameter, the distance between
133 heat station and demand points, the temperature difference between supply and return water,
134 pressure loss, outdoor temperature have an impact on heat losses. Trade-offs between these
135 parameters must be analyzed to minimize heat loss.

136 The biomass supply chain comprises nine main consecutive steps: Cultivation, harvesting,
137 loading, raw material transportation, unloading, warehousing, pretreatment, conversion to energy
138 and end-product transportation. The baling and shredding (size reduction) sub-processes can be
139 included to supply chain according to a given case. All processes except for cultivation,
140 harvesting, loading, raw material transportation can take place in a trigeneration system.
141 Minimizing any kind of losses between these successive processes calls for optimization
142 technics.

143 Decisions on biomass to energy supply chain have been dealt with strategic, tactic and
144 operational levels. The strategic level includes long-term decisions like the selection of site,
145 capacity, technology, transportation node, biomass suppliers, and preprocessing facilities. Once a
146 strategic decision is made, it is very unlikely to be altered in the short term (Yue and You 2016).
147 Geographic Information Systems (GIS) has effective tools for all three levels, particularly at the
148 strategic level.

149 Within the concert of renewable energy technologies, bioenergy can play a decisive role during
150 the next decades, when smartly designed and applied under favorable conditions. In this respect,
151 an efficient and effective supply chain and logistics management represents one key parameter
152 (Turkenburg 2000). Efficient supply chain management and optimization is a very complex
153 problem. To solve the sustainable biomass supply chain management problem, mathematical
154 optimization modeling, heuristic or meta-heuristic solution technics can be analyzed with
155 understanding the concept of biomass to bioenergy routes.

156
157
158

159 **3. Materials and methods**

160 **3.1. Heuristic method**

161
162 Unlike mathematical modeling, heuristic or meta-heuristics do not guarantee a globally optimal
163 solution, however, they are very fast in complex problems such as NP-hard and NP-complete
164 problems. They can optimize problems with non-linear, non-convex and non-continuous
165 functions in a reasonable amount of time. Also, meta-heuristics, which are generally inspired by
166 natural and physical events, is known as the most sophisticated heuristics. A heuristic is specific
167 to the problem, while meta-heuristic can be applied to all kinds of problems. Heuristics may stick
168 in local optimums and cannot be used in various types of problems, whereas meta-heuristic has
169 ways out of local optimums and can be used in a wide range of problems (Ghaderi et al. 2016).
170 As the size of the problem increases in combinational problems, the computational time of
171 finding good or best solutions increases exponentially as well. Meta-heuristic algorithms can find
172 near-optimum solutions for complex and large-scale problems in a short time.

173 Celli et al. (2008) used a GIS-based genetic algorithm to determine the number, capacity, and
174 location of biogas facilities and applied the algorithm to a region in Italy. The objective function
175 in the model is maximizing the profitability of the investment. Sultana and Kumar (2012)
176 presented a location-allocation model embedded in GIS and applied it to a region in Canada.
177 They used the Analytic Hierarchy Process (AHP) technic to identify the weight of predefined
178 criteria for the selection of a pellet plant. After determining the number of candidate sites, the p-
179 median solver method was employed in GIS to minimize the total biomass transportation cost.
180 Reche-Lopez et al. (2009) used four meta-heuristics to determine the optimal placement and
181 supply area of power plants and then compared solutions. All meta-heuristics were applied with
182 experimental data. The profitability index was considered as the objective function. GIS was
183 employed to divide the region into parcels with a constant surface of 2 km² and to provide the
184 required data for optimization parameters. Rentizelas et al. (2009) modeled the bioenergy supply
185 chain wherein the trigeneration system and district heating and cooling system were employed to
186 make use of energy with an efficiency of almost 90%. The model was applied to a region in
187 Greece to demonstrate its inherent capabilities. They considered five biomass types as feedstock
188 (3 herbaceous and 2 woody out of which) and a single power plant to maximize the net present
189 value of the potential investment by determining the optimal size, location, types and amounts of
190 biomass to be used in a power plant. Vera et al. (2010) proposed a Binary Honey Bee Foraging
191 algorithm that determines the capacity, location and supply area of biomass power plants. The
192 objective function was formulated as maximization of investment profitability. The whole terrain

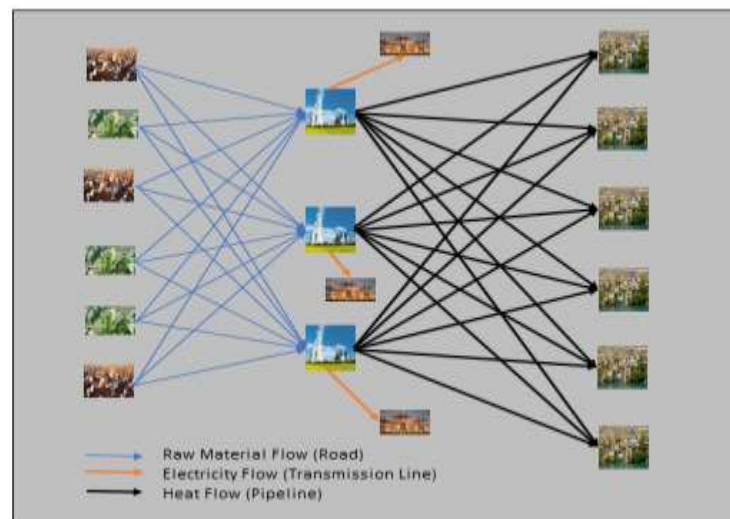
193 was divided into square-shaped cells in GIS. The centroids of each cell were identified as a
194 candidate plant site.

195 In this study, as a solution technic, the simulated annealing algorithm was applied to biomass to
196 bioenergy and reviewed in the literature survey. Especially, GIS based heuristic studies were
197 examined and employed together with metaheuristic solution technics in some studies to
198 simulate the actual case in a better way. GIS was also used exclusively as a site selection tool to
199 determine suitable locations, particularly in waste management. However, these studies which
200 are not integrated with heuristic algorithms such as SA were not addressed in the literature
201 review. To the best of our knowledge, This is the first study on determination of biomass power
202 plant location using GIS based-simulated annealing algorithm.

203 3.2. Problem definition

204
205 The general framework of this problem is different from our published study (Akgül and
206 Seçkiner 2019). In this study, GIS tools were employed exactly to show the actual case and used
207 a heuristic instead of mathematical modeling. Figure 1 demonstrates a schematic design of a
208 bioenergy supply chain.

209



210

211 Figure1. A basic illustration of biomass to bioenergy supply chain [2]

212

213 3.3. Geographic information system (Spatial analysis)

214 In this section, a suitability model that was developed for the biomass to bioenergy supply chain
215 design was introduced. This section aims to propose a model in a GIS environment for a
216 selection of the most suitable candidate lands that were suited to a power plant building. The

217 selection process was carried out according to some preference criteria. ArcGIS software was
218 employed for suitability analysis. The suitability model was applied to Bismil District in
219 Diyarbakır Turkey.

220 Sitting a bioenergy facility in both the most suitable land and optimum location has crucial
221 importance in the bioenergy sector. Selecting the most suitable land according to a set of
222 particular criteria may reduce initial investment and operation costs. At the same time, it may
223 boost annual revenues. In this regard, GIS is a powerful tool for determining the optimum
224 location and selecting the most suitable lands. GIS is defined as collecting, storing, transforming,
225 analyzing and visualizing spatial data obtained from the real world for a certain purpose
226 employing some software tools and methods. Information systems built for the analysis of spatial
227 data provide great convenience to policymakers in decision-making processes for the solution of
228 complex social, economic and environmental problems experienced by human beings, as well as
229 saving time, money and personnel (Goodchild 1997). The major components of the GISs are
230 hardware, software, personnel, geographic data, and methods.

231 The GIS allows carrying out an advanced analysis like network and suitability analysis by using
232 the topological properties of objects in the real world. To put it simply, traditional maps get
233 smart thanks to GIS. GIS is capable of finding the optimal solution of location-allocation
234 problems utilizing network analysis tools. Optimal size and location may be found by the
235 utilization of network analysis tools depending on the size and type of the problem. However,
236 our problem is highly complex. Thus, location-allocation analysis embedded in GIS could not be
237 utilized. Instead, a meta-heuristic model was used to determine the optimum number, size, and
238 locations of the power plant(s) and it's/their demand point/s (settlement) for providing heat. For
239 this purpose, a meta-heuristic-based algorithm programmed in Excel Visual Basic Applications
240 (VBA) was proposed. Real data, which was used in the proposed algorithm, was obtained
241 through suitability analysis carried out in GIS.

242 As aforementioned, the proposed model was applied to Bismil District, Diyarbakır (Turkey) as a
243 case study. Agricultural activities are very common in Bismil. A surface area of 1.737 km² is
244 devoted to agriculture and 60% of which is irrigable. According to a published study (Alibaş, et
245 al. 2015), Bismil ranks first in herbal production among the other districts of Diyarbakır. Wheat,
246 barley, lentil, cotton, and corn are cultivated in the agricultural land of Bismil. Cotton and corn
247 are generally grown in irrigable areas (on the south part), while grain crops are grown in dry
248 areas (on the north side). Agricultural parcels and candidate power plant locations were
249 represented as a polygon, centroid coordinates of these polygons were represented as point and

250 distance matrixes were represented as a line in GIS. Vector data and raster data types were used
251 in the proposed model.

252 The centroid points of the agricultural parcels were considered as a raw material supply point.
253 The points (centroid coordinate of the polygon) revealed as a result of land suitability analysis
254 were considered as candidate power plant points and residential areas whose household is greater
255 than 40 were taken as the hot and cold heat demand points. The electricity generated in the
256 power plant was transmitted to the nearest high voltage line. Therefore, the Euclidean distance
257 matrix from the centroid points of the parcels to the candidate power plant points, from the
258 power plants and to the electricity line and the settlements were created.

259

260 3.4. Current situation

261

262 There are villages, main roads, rivers, high voltage electricity transmission lines, and water
263 channels on the overall Bismil map as shown in Figure 2a. Cotton and corn are grown on the
264 irrigable land, which covers the south part of the reference line as given in Figure 2b.
265 Agricultural parcels in which only cotton and corn are grown were considered as a raw material
266 supply point. Thus, parcels, which are in the south of a reference line, which is 10 km north of
267 the water channel, were taken. On the other hand, the entire Bismil map was considered for
268 determining candidate power plant points and settlements. A power plant can be established in
269 the north or south part of the reference line or a settlement located in the north or south part of
270 the reference line can get heat energy. However, parcels in the south part of the reference line
271 can be a supply point as cotton and corn can be grown in these parcels.

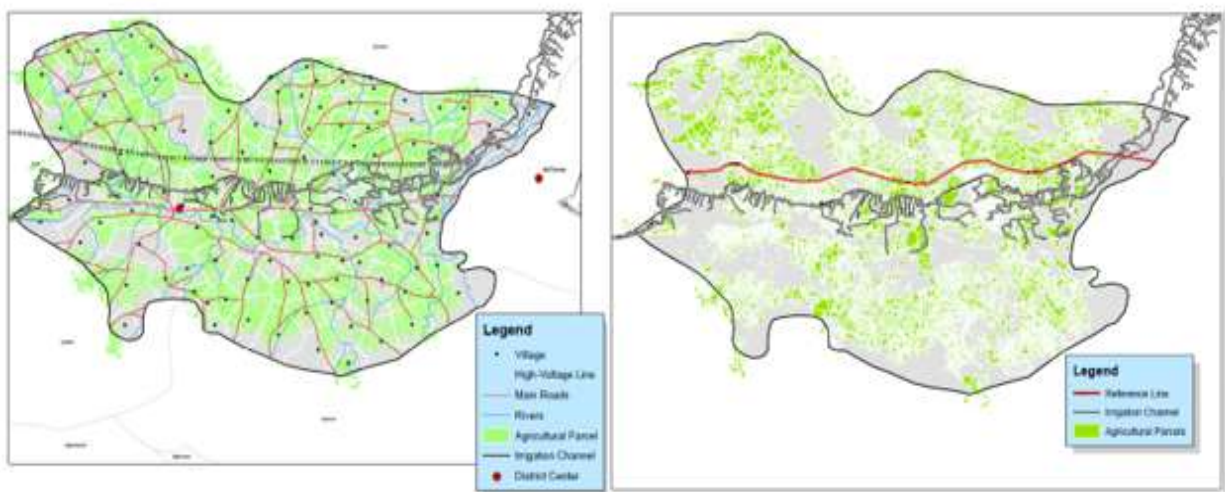


Fig. 2. Current situation (a,b)

274 **3.5. Land suitability analysis**

275
276 The geographical information system has spatial analysis tools to draw meaningful conclusions
277 from the map data. At this point, the suitability analysis used in site selection analysis was
278 applied to the agricultural terrain of Bismil, Diyarbakır, Turkey to determine the suitable
279 candidate power plant locations. The suitability analysis consists of two sub-analyses called
280 suitability model and restriction model. The formulation of the suitability analysis is as follows
281 in Equation 1.

$$282 \quad s_i = \prod_{j=1}^m r_j \sum_{i=1}^n w_i C_i \quad (1)$$

283 Where

284 s_i = Suitability index

285 r_j = Boolean value (0,1) of j^{th} criteria in restriction model

286 m = Number of the criteria in the restriction model

287 w_i = Weight assigned to the i^{th} preference criteria in suitability model

288 C_i = Value of the i^{th} preference criteria in suitability model

289 n = Number of the preference criteria in suitability model

290
291 In Equation 1, the restriction model is set by giving Boolean value (0,1) to certain criteria (j).
292 The restricted cells (90x90 m) are represented by 0, while viable cells are represented by 1. As
293 for in the second part, the suitability model is set by giving weights to certain criteria (i). In the
294 next stage, both layers (suitability and restriction) are overlaid (multiplied) and the grid (raster)
295 cells whose suitability analysis result (s) equals to zero are excluded. This means that these grid
296 cells are not suitable according to a certain criterion. In other words, grid cells whose suitability
297 values are greater than zero are considered as suitable. Equation 1 is applied to all the cells. After
298 that, the most suitable ones among the suitable lands are selected based on a certain criterion
299 (suitability value of the cell, the size of the land).

300 **3.5.1. Restriction model**

301
302 In the restriction model, the soil map layer and water body layer obtained from the Ministry of
303 Agriculture and Forestry and General Directorate of State Hydraulic Works in Turkey were
304 utilized. The restriction model aims to restrict the selection area as much as possible and fulfills

305 some legislative and environmental obligations. The excluding criteria were demonstrated in
 306 Table 1. The location of the bioenergy facility must be at least 250 meters away from the
 307 settlements due to renewable energy law. Facility location must be also at least 150 meters away
 308 from water bodies such as lake, river and irrigation channels. This constraint enables facility
 309 infrastructure more durable. The two buffer zones were established to meet constraints. Land-use
 310 types such as inadequate drainage, flood plains, vineyards and olive groves on the soil map layer
 311 were excluded in the model. All these limitations were coded on the raster cells with a size of
 312 90x90 m through Boolean values. The excluding and including cells were revealed by
 313 multiplying the related raster layers using Equation 2.

$$314 \quad rv = (r_{buffer(settlement)}r_{buffer(water)}r_{soil\ map}) \quad (2)$$

315 Where rv represents the restriction value of the cell. $r_{buffer(settlement)}$, $r_{buffer(water)}$ and $r_{soilmap}$ denote
 316 the boolean value of three criteria, respectively. For instance, if a cell is 250 m far away from the
 317 settlement, then its value takes 1 as it is viable for the construction of a power plant in the
 318 restriction model.

319 Table 1. The set of exclusion criteria used in restriction model

Settlement	Water	Soil Map
250 m (buffer)	150 m (buffer)	"DCV IN ('YR' , 'YT')", "DTO IN ('y') OR SAK IN ('S' , 'V' , 'Vs' , 'B' , 'Bs' , 'O' , 'Za' , 'Zç' , 'Zz' , 'Zf' , 'Zk' , 'Zm' , 'Zt' , 'Zp' , 'Zi' , 'Zd') OR AZT IN ('Y' , 'SB' , 'DK') OR AKK IN ('I' , 'II') OR ATS IN ('w') OR DCV IN ('GL' , 'HV' , 'IR' , 'KY' , 'MZ' , 'YR' , 'YS' , 'YT')"

320
 321
 322 **3.5.2. Suitability model**
 323
 324 In the suitability model, six preference criteria were weighted according to importance. The
 325 distribution of weightiness was determined according to expert judgments. In such cases, the
 326 Analytic Hierarchy Process (AHP) method, which is one of the multi-criteria decision-making
 327 processes, can be utilized to calculate weight values more scientifically. Proximity to supply
 328 points, settlement, main roads and water bodies raster layer, slope raster layer and land use raster
 329 layer was employed as an input in this model. The six input rasters were reclassified to a
 330 common measurement scale of 1 to 10. 10-point denotes the most favorable preference and vice
 331 versa. Each raster layer cell's value was multiplied by a weight of related raster layer and all
 332 raster layer datasets were combined to create a weighted overlay layer. The formulations of the

333 suitability model as given in Equation 3 and the weights of the criteria set as given in Table 2
 334 were shown as follows.

$$335 \quad sv = \sum_{i=1}^n w_{proximitytosupplypoints} C_{psp} w_{proximitytosettlement} C_{ps} w_{slope} C_s w_{proximitytomainroads} C_{pmr}$$

$$336 \quad w_{landuse} C_{lu} w_{proximitytowaterbodies} C_{pwb} \quad (3)$$

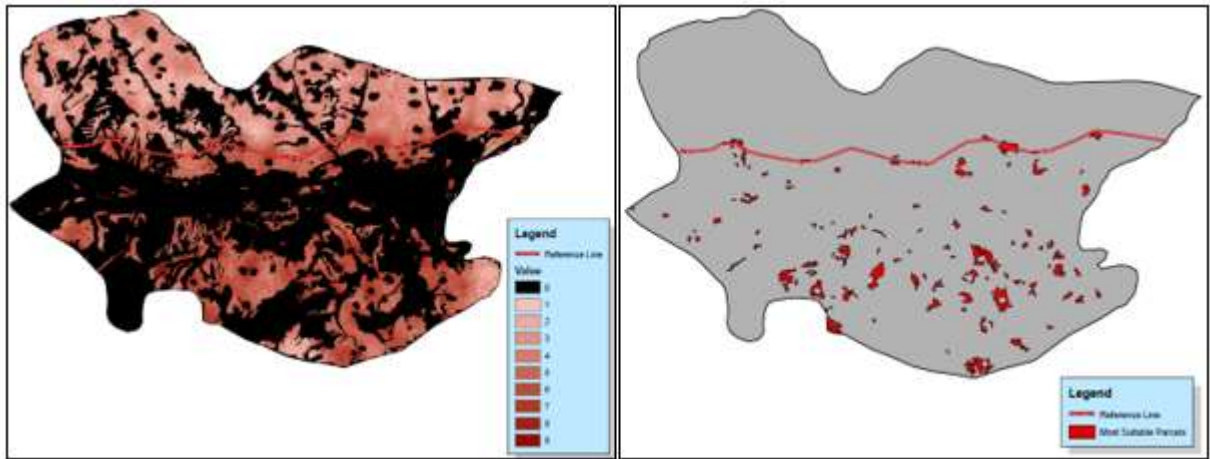
337 Where *sv* represents the suitability value of the cell. *wproximitytosupplypoints*, *wproximitytosettlement*, *wslope*,
 338 *wproximitytomainroads*, *wlanduse* and *wproximitytowaterbodies* are weight of criteria and indicated in Table 2. *c_{psp}*,
 339 *c_{ps}*, *c_s*, *c_{pmr}*, *c_{lu}* and *c_{pwb}* denote cell value of every criterion. This value is calculated through data
 340 classification methods in ArcGIS.

341 Table 2. Preference criteria and weights

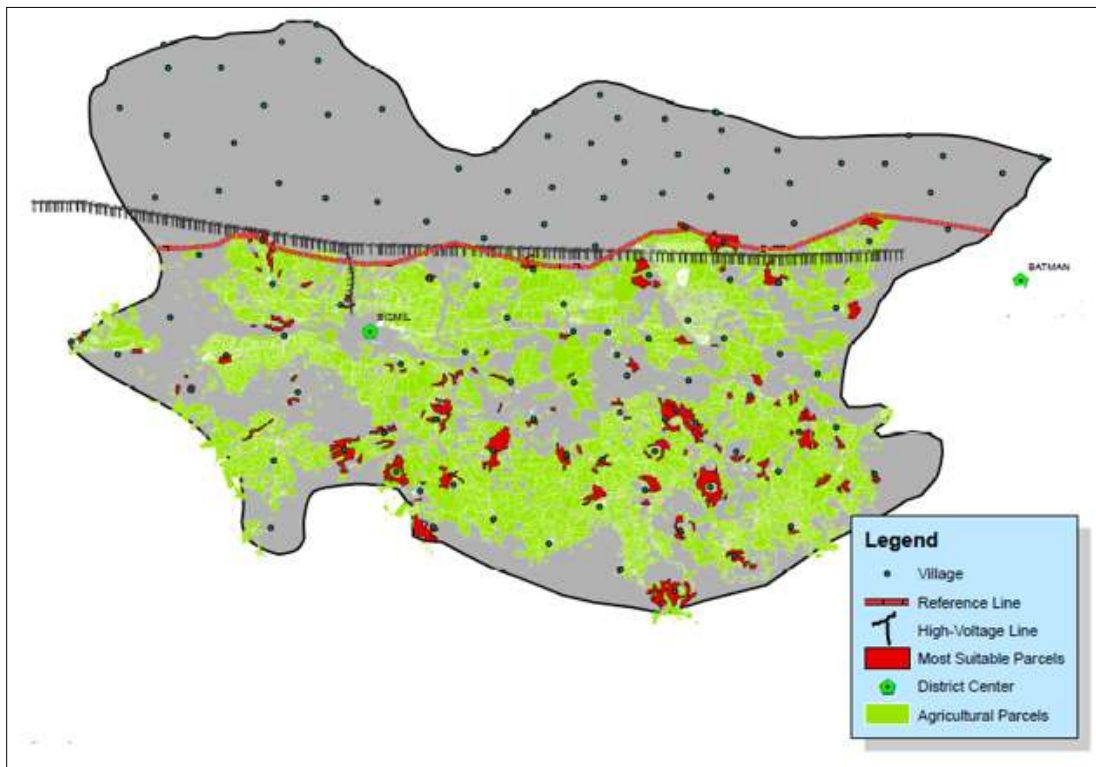
Proximity to Supply Points	Proximity to Settlements	Slope	Proximity to Main Roads	Land Use	Proximity to Water Bodies
35%	20%	5%	15%	15%	10%

342
 343 **3.5.3. Final suitability model and most suitable parcels**
 344
 345 Multiplying the final restriction raster layer and weighted overlay raster layer created the final
 346 suitability layer. Each raster layer cell with a value of zero in the restriction model was also
 347 excluded in the final suitability model as expected. The final suitability map is shown in Figure
 348 3a as follows. As can be noticed, the suitable areas are clustered mostly in the south of the
 349 reference line due to the high percentage of criteria of proximity to supply points and proximity
 350 to water bodies.

351 After creating the final suitability raster layer, areas with preference scores of 7, 8, 9 and 10 and
 352 with a cover area of more than 4 ha were determined as the most suitable candidate points for
 353 power plant building. Raster data type was used for scoring preference criteria and vector data
 354 (polygon) was used for calculation of the coverage area of separate parcels. Therefore, after the
 355 completion of the scoring evaluation, the raster layers were converted to polygons for cover area
 356 calculation. According to the predefined criteria (suitability score and surface area), 127
 357 polygons (parcel) were determined as the most suitable lands for power plant construction (see
 358 Figure 3b). In other words, there are 127 candidate locations on which a power plant can be
 359 constructed.



360
 361 Figure 3. Final suitability map (a), the most suitable parcels (b)
 362 The analysis was completed by incorporating high transmission voltage lines in the model. The
 363 settlements shown in Figure 4 whose household number is greater than 40 were considered hot
 364 and cold heat demand points in the model. The Euclidean distances between the candidate power
 365 plant points and agricultural parcels, candidate power plant points and electricity transmission
 366 line, candidate power plant points and settlements were retrieved from the GIS to be employed
 367 as a parameter in the meta-heuristic model. The final design in GIS was demonstrated in Figure
 368 4.



369
 370 Figure 4. The final design of the proposed GIS model
 371 There are 14,391 parcels and 50 settlements whose population is greater than 50 based on the
 372 data retrieved from GIS. Some parcels have a quite small surface area. Therefore, parcels whose

373 surface area is greater than 20 da were considered not to reduce the efficiency of raw material
374 transportation. Thus, the number of parcels are considered in meta-heuristic decreased 7,784,
375 which covers almost a surface area of 900,000 da. Eventually, 2 distance matrixes with a size of
376 7,784 x 127, 50 x 127 and a vector with a size of 127 x 1 representing parcels to power plants,
377 settlements to power plants and power plants to the nearest high voltage transmission line were
378 created based on the results of the analyses carried out in GIS.

379 **3.6. Finding the best plant: a case study based on Simulated Annealing**

380 In this section, a simulated annealing heuristic algorithm was developed and applied to Bismil
381 District in Diyarbakır, Turkey. At first, the optimization rate of the proposed heuristic was found
382 by applying it to a small-sized problem, which was solved via a MILP model (Akgül and
383 Seçkiner 2019). After observing that the viability of the simulated annealing heuristic is
384 satisfactory, the actual problem was solved based on the actual data retrieved from GIS.

385

386 **3.6.1. Simulated annealing algorithm**

387 Simulated annealing (SA) algorithm was developed by Kirkpatrick et al. (1983). The proposed
388 SA algorithm based on the previous algorithm developed by Metropolis et al. (1953). This
389 algorithm simulates the heating and cooling process of a material called annealing. Annealing
390 refers to an analogy with metallurgy. The solid material is heated and slowly cooled back under
391 controlled conditions to improve the strength and durability of the material. At the end of the
392 process, the energy of the atoms decreases, and the structure of the solid material becomes
393 stable. This shows that atoms in the solid material do not move anymore beyond a certain
394 temperature, which refers to the local or global optimum point in the SA algorithm.

395 SA is a probabilistic meta-heuristic due to having a random initial solution and utilizing a
396 probability when the neighborhood solution is worse than the current solution. The initial and
397 final temperature and gradual cooling rate are taken into account in the annealing process. Better
398 solutions are always accepted unconditionally as expected. Some uphill moves (downhill for
399 maximization), which represent the worse solution, can escape local optima through a
400 probability of $e^{-(S_n - S_c)/T}$, where T is the current temperature, S_c is the current solution
401 (energy) and S_n is the neighbor solution (energy). SA differs from a hill-climbing search
402 algorithm due to making use of this probability to escape local optimal. In such cases where the
403 algorithm finds a worse solution, a uniform random number between 0 and 1 is generated. If that
404 number is less than the probability value, the worse solution is accepted in case there might be
405 better solutions beyond this point. As might be observed from the probability formula, as the

406 temperature decreases (towards the end), and change in energy decreases, the formula output
407 becomes smaller. So, the chance of accepting worse solutions is decreased. This also means that
408 the system becomes stable towards to end. While the temperature is high, the algorithm can jump
409 out of any local optimums. The higher an initial temperature is determined, the better exploration
410 in the entire search space. However, a high initial temperature increases the computation time.

411 SA was initially developed for combinatorial problems and then adapted for continuous
412 problems. The unique advantages of SA are its ability to escape from local optima,
413 straightforward implementation, and rapid convergence. In a SA algorithm, the most important
414 factors are initial temperature, the number of moves allowed at each temperature, the cooling
415 rate, and the final temperature at which the search is completed (Castillo-Villar 2014). They are
416 called as control parameters. These parameters should be adapted to the problem dealt with, as
417 the search landscape can be different in every single problem. Besides, fine tunings can be
418 adjusted at a particular step in the algorithm. All these adjustments allow the algorithm to escape
419 local optimums and to find a better solution.

420 Notations used in SA and their pseudo-codes are demonstrated as follows.

421 **Notations:**

422 X_0 = Initial random solution

423 X_i = Current solution

424 X_{i+1} = Potential (Neighbor) solution

425 X_b = Best solution

426 T_0 = Initial temperature

427 T_t = Temperature at stage t

428 T_f = Final temperature

429 a = Cooling rate

430 N_n = Number of moves at each temperature

431 σ = Move operator

432

433 **Pseudocode for simulated annealing**

434 Step 1: Set X_0 , T_0 , T_f , a , N_n and σ

435 Step 2: Start at a random point in the search space

436 Step 3: $X_b = X_i$

437 Step 4: Move to another location by using the move operator, σ

438 Step 5: Look neighborhood points around the current solution point and move to one of these
439 points,

440 $n = 1$
 441 Step 6: If $f(X_{i+1})$ is better, take it as current solution, $X_i = X_{i+1}$
 442 If $f(X_i)$ is better than $f(X_b)$, $X_b = X_i$
 443 Step 7: If not, generate a random number between 0 and 1 and check the random number is
 444 less than $e^{\frac{-(f(X_{i+1})-f(X_i))}{Tt}}$
 445 Step 7.1: If less, take it as the current solution, $X_i = X_{i+1}$
 446 Step 7.2: If greater, don't take it and stay where you are and look around the current
 447 point
 448 Step 7.3: $n = n + 1$
 449 Step 8: Repeat steps 5 to 7 while $n \leq N$
 450 Step 9: $T_{i+1} = a \times T_i$
 451 Step 10: Repeat steps 5 to 9 while $T_i \leq T_f$
 452 Step 11: Return X_b

453
 454 There are 7,784 parcels and 50 settlements and 127 candidate power plant sites in the actual
 455 problem. Raw materials are transported from the parcels to the power plant and after processing
 456 in a power plant, generated electricity is transmitted to the nearest high voltage power line, and
 457 heat is transferred to settlements. The algorithm, which runs while moving neighbor point from
 458 the current point (fifth step in pseudo-code) demonstrated as follows;

- 459 • Select a set of random power plants as an initial solution
- 460 • Transport raw material from the parcel to the nearest location where a power plant
461 established
- 462 • Transfer hot heat produced from the power plant/s to the settlement which has the highest
463 heat demand¹
- 464 • If remained hot heat produced from power plant/s is greater than the highest heat demand
465 among the settlement which has not received hot heat, transfer hot heat to the settlement
466 which has the highest heat demand among the settlement which has not received hot heat
467 yet
- 468 • Repeat the fourth step until remained hot heat is less than the highest heat demand among
469 the settlement which has not received hot heat
- 470 • Transfer remained hot heat to the settlement which has the highest heat demand among
471 the settlement which has not received hot heat

¹ Monte Carlo Simulation was employed to determine which strategy is more attractive. The result indicates that providing heat to settlements in descending heat demand order is more convenient than ascending order.

- 472 • Transfer cold heat produced from the power plant to the settlement which already
473 received hot heat
- 474 • If remained cold heat greater than the highest cold heat demand among the settlement
475 which has not received cold heat, transfer cold heat to the settlement which has the
476 highest cold heat demand among the settlement which has not received cold hot heat yet
- 477 • Repeat the eighth step until remained cold heat is less than the highest cold heat demand
478 among the settlement which has not received cold heat
- 479 • Transfer remained cold heat to the settlement which has the highest heat demand among
480 the settlement which has not received cold heat
- 481 • Transmit electricity from the power plant to the nearest high voltage line
- 482 • Calculate the net present value

483 It was allowed that partial demand of the settlement could be satisfied. If a pipeline network is
484 constructed between the power plant and settlement for hot or cold energy transmission and if
485 there is remainder heat, it can be sold the settlement for which a pipeline network exists.

486

487 **3.6.2. Assumptions**

488

489 In this study, the average amount of agricultural residue of two years was considered for every
490 year in the project lifetime. Thus, there will be the same amount of income and outcome (cash
491 flow) for every year in this study. However, cash flow was considered a fixed value combining
492 two successive years in the project lifetime in the previous study. Accordingly, project lifetime
493 was considered as 20 years and the discount rate was taken as 10.914 in this study. Aside from
494 this difference, two assumptions were included existed assumptions as described in our previous
495 study (Akgül and Seçkiner 2019). The first assumption is that raw material in a parcel is allowed
496 to transport only one power plant. It means a parcel can be assigned just one power plant. The
497 second assumption is that a settlement is allowed to receive heat from just one power plant.

498

499 **3.6.3. Indices, parameters, equations and control parameters**

500

501 Indices and parameters were given in our published study (Akgül and Seçkiner 2019). 7784
502 parcels, 127 candidate power plant points and hot and cold energy demand points are represented
503 as *j*, *k* and *l* indices respectively in this study. The parameters are exactly as same as the

504 parameters given in that cited study. We invite readers to read our previous study to eliminate the
505 repetition of too many similar parameters in this study. Apart from those parameters specific to
506 our previous study, some extra parameters were determined in this study due to the first
507 assumption mentioned in the section of 6.2.1. Additional parameters were indicated as follows;

508 Additional Parameters:

509 C_{kj} and G_{kj} : The annual average amount of the hot/cold heat obtained by the k^{th} settlement from
510 the power plant at the j^{th} candidate point. The annual average amount of the hot/cold heat is
511 calculated based on the produced amount of hot/cold heat in the first and second year,

512 F_{kj} = It equals to 1 if k^{th} settlement gets the hot or cold heat from the plant located at the j^{th}
513 candidate point, 0 otherwise,

514 IP_j : Annual average installed power of power plant established in the j^{th} candidate point (MW).
515 Annual average installed power is calculated based on the generated power in the first and
516 second year

517 K_{ij} = It equals to 1 if the raw material is transported from i^{th} parcel to the plant located at j^{th}
518 candidate point, 0 otherwise,

519 Ma_{kkj} : The unit amount of hot and cold heat flow between k^{th} settlement and power plant at the
520 j^{th} candidate point ($\text{MW}_{\text{heat}}/\text{h}$). If a settlement gets hot and cold heat, a greater amount is
521 considered to construct pipeline as expected

522 SA_i : Annual average supply amount of the raw material from the i^{th} parcel (ton), $SA_i = PA_i X$

523
$$\frac{YPSK_{1i} + YPSK_{2i}}{2}, i = 1 \dots 7784,$$

524 X_{kj} = It equals to 1 if k^{th} settlement gets hot heat from the plant located at the j^{th} candidate point,
525 0 otherwise,

526 Y_{kj} = It equals to 1 if k^{th} settlement gets cold heat from the plant located at the j^{th} candidate point,
527 0 otherwise,

528
529 Here, the low heating value of the agricultural products (LHV), the yield of those products per
530 km^2 (YPSK), organic dry matter rate of those products (ODMR) and unit raw material price of
531 those products (URMP) were given in Table 3. This table can be regarded as a crop pattern of the
532 whole agricultural land handled in this study. This cropping pattern is repeated interrelated
533 through project lifetime. It means that if corn is cultivated on the i^{th} parcel in the first year, cotton
534 will be cultivated in the second year on the same parcel.

Table 3. Harvested crops and their attributions

Parcel No	PA _i	Type of the agricultural crop harvested in the first year	Type of the agricultural crop harvested in the second year	YPSK _{1i} (ton/km ²)	YPSK _{2i} (ton/km ²)	ODMR _{1i} (%)	ODMR _{2i} (%)	LHV _{1i} (Mwh/ton)	LHV _{2i} (Mwh/ton)	URMP _{1i} (euro/ton)	URMP _{2i} (euro/ton)
i ₁	80	Cotton	Corn	0,30	0,25	0,50	0,85	4,78	4,68	20	40
i ₂	55	Corn	Cotton	0,25	0,30	0,85	0,50	4,68	4,78	40	20
i ₃	80	Cotton	Corn	0,30	0,25	0,50	0,85	4,78	4,68	20	40
...
i ₇₇₈₄	89	Corn	Cotton	0,25	0,30	0,85	0,50	4,68	4,78	40	20

536

537 Equations:

538 Approximately an installed power of 29 MW can be produced from corn and cotton residues in
539 the field based on the real data. Distribution of the whole power to candidate power plants is
540 determined by the SA algorithm through comparing trade-offs between various inputs such as
541 transportation cost of raw material, transmission cost of heat and electricity, the unit installation
542 cost of the power plant and pipeline network. Seasonal fluctuations were considered for
543 calculation of power plant and pipeline network installation cost.

544 Installed power is calculated in Equation 4 given as follows:

$$545 \quad IP_j = \begin{cases} 0 & , K_{ij} = 0 \\ \left(\sum_{i=1}^{7784} \frac{(SA_{1i} * LHV_{1i} + ODMR_{1i}) + (SA_{2i} * LHV_{2i} + ODMR_{2i})}{2} \right) \times EE \times GE \times \frac{RMDR}{OH} & , K_{ij} = 1, j = 1 \dots 127 \end{cases} \quad (4)$$

546 Power plant installation cost is calculated in Equation 5 given as follows:

$$547 \quad PPIC_j = \begin{cases} 0 & , IP_j = 0 \\ 3.975.198,31 + 568.456,61 \times IP_j \times EHDR & , IP_j > 0, j = 1 \dots 127 \end{cases} \quad (5)$$

548 Power plant total installation cost is calculated in Equation 6 given as follows:

$$549 \quad PPTIC = \sum_{j=1}^{127} PPIC_j \quad , \quad (6)$$

550 Power plant annual average operation and maintenance cost is calculated in Equation 7 as
551 follows:

$$552 \quad PPOMC = PPTIC \times PPOMCR, \quad (7)$$

553 Power line installation cost per kilometer from the k^{th} settlement to the j^{th} candidate power plant
554 point, which is generated from a regression model based on unit flow, and DSP_{k,j}, is calculated in
555 Equation 8 as follows:

$$556 \quad \text{PLICPK}_{kj} = \begin{cases} 0, & F_{kj} = 0 \\ 8.193,78 + 3.586,11 \times \text{Mak}_{kj} \times \text{EHDR}, & F_{kj} = 1, k = 1 \dots 50, j = 1 \dots 127 \end{cases} \quad (8)$$

557 Power line network total installation cost and annual average power line network operation and
558 maintenance cost are calculated in Equation 9 and 10 given as follows:

$$559 \quad \text{PLNTIC} = \sum_{k=1}^{k=50} \sum_{j=1}^{j=127} \text{PLICPK}_{kj} \times \text{DSP}_{kj}, \quad (9)$$

$$560 \quad \text{PLNOMC} = \text{PLNTIC} \times \text{PLOMCR}, \quad (10)$$

561 Electricity transmission total installation cost is calculated in Equation 11 given as follows:

$$562 \quad \text{ETTIC} = \begin{cases} \left(\sum_{j=1}^{j=127} \text{DPETL}_j \times \text{ETLICPK} \right) + 2.000.000,00, & 0 < IP_j \leq 20, \\ \left(\sum_{j=1}^{j=127} \text{DPETL}_j \times \text{ETLICPK} \right) + 2.800.000,00, & IP_j > 20, \\ 0, & IP_j = 0 \end{cases} \quad (11)$$

563 Annual average raw material transportation cost is calculated in Equation 12 given as follows:

$$564 \quad \text{RMTC} = \begin{cases} 0, & K_{ij} = 0 \\ \left(\sum_{i=1}^{i=7784} \sum_{j=1}^{j=127} \text{DPP}_{ij} \times \text{SA}_i \right) \times \text{URMTC}, & K_{ij} = 1 \end{cases} \quad (12)$$

565 Annual average hot and cold heat transportation cost is calculated in Equation 13-14 given as
566 follows:

$$567 \quad \text{HHETC} = \begin{cases} 0, & X_{ij} = 0 \\ \left(\sum_{k=1}^{k=50} \sum_{j=1}^{j=7} C_{kj} \times \text{DSP}_{kj} \right) \times \text{HTCPK}, & X_{ij} = 1 \end{cases} \quad (13)$$

$$568 \quad \text{CHETC} = \begin{cases} 0, & Y_{ij} = 0 \\ \left(\sum_{k=1}^{k=50} \sum_{j=1}^{j=127} G_{kj} \times \text{DSP}_{kj} \right) \times \text{HTCPK}, & Y_{ij} = 1 \end{cases} \quad (14)$$

569 Annual average electricity loss cost through transmission is calculated in Equation 15 given as
570 follows:

$$571 \quad \text{ETLLC} = \begin{cases} 0, & IP_j = 0 \\ \sum_{j=1}^{j=127} \left(IP_j \times \text{EP} \times \text{OH} \times (1 - \text{ECRIP}) \right) \times (1 - \text{ELM}_j), & IP_j > 0 \end{cases} \quad (15)$$

572 Annual average raw material cost is calculated in Equation 16 given as follows:

$$573 \quad \text{RMC} = \sum_{i=1}^{i=7784} \frac{\text{SA}_{1i} \times \text{URMP}_{1i} + \text{SA}_{2i} \times \text{URMP}_{2i}}{2}, \quad (16)$$

574 Annual average revenues from electricity sale, hot heat sale, cold heat sale and fertilizer sale are
575 calculated Equation 17-20 given as follows:

$$576 \quad \text{ES} = \sum_{j=1}^{j=127} IP_j \times \text{EP} \times \text{OH} \times (1 - \text{ECRIP}), \quad (17)$$

$$577 \quad \text{HHES} = \begin{cases} 0, & X_{ij} = 0 \\ \left(\sum_{k=1}^{k=50} \sum_{j=1}^{j=127} C_{kj} \times \text{RHRAL}_{kj} \right) \times \text{HHEP}, & X_{ij} = 1 \end{cases} \quad (18)$$

$$578 \quad \text{CHES} = \begin{cases} 0, Y_{ij} = 0 \\ (\sum_{k=1}^{50} \sum_{j=1}^{127} G_{kj} \times \text{RHRAL}_{kj}) \times \text{CHEP}, Y_{ij} = 1 \end{cases} \quad (19)$$

$$579 \quad \text{FS} = \left(\sum_{i=1}^{7784} \frac{SA_{1i} \times \text{ODMR}_{1i} + SA_{2i} \times \text{ODMR}_{2i}}{2} \right) \times \text{RMDR} \times \text{FR} \times \text{FP}, \quad (20)$$

580 Power plan initial variable cost, annual average electricity sale, fertilizer sale, and raw material
581 cost are pre-calculated as they are independent of supply chain design. For this reason, these
582 costs and income items were excluded in the SA algorithm.

583 Control Parameters :

584 As abovementioned, control parameters determine the viability of the SA algorithm. They should
585 be adjusted according to the case. In this study, initial temperature and final temperature were
586 determined based on the formulas presented in a published study (Seçkiner 2005).

587 Initial temperature (T_0) was calculated in Equation 21 given as follows:

$$588 \quad T_0 = \frac{f_{max} - f_{min}}{\ln P_i} \quad (21)$$

589 Where f_{max} and f_{min} represent the maximum and minimum value of the fitness function, P_i
590 represents the acceptance probability of the solutions at the initial temperature. The final
591 temperature was calculated similarly based on P_f which represents the acceptance probability of
592 the solutions at the final temperature.

593 Temperature is reduced geometrically based on formula demonstrated in Equation 22 given as
594 follows. Every change in temperature denotes iteration in the SA algorithm.

$$595 \quad T_{t+1} = T_t \times a \quad (22)$$

596 In the beginning, the initial temperature is taken as a high value and a few hundred moves are
597 carried out at this temperature (Kirkpatrick 1983). The probability score (P_i), which is given by
598 the user at the beginning, is compared to the ratio of accepted moves to all attempted moves. If
599 P_i is greater than the ratio, this temperature is considered initial temperature; otherwise,
600 multiplying two increases initial temperature value. This approach was employed for the
601 calculation of the initial temperature in the proposed meta-heuristic. The final temperature can
602 be calculated similarly.

603 **3.6.4. Fitness Function**

604
605 As abovementioned, factors that do not affect the solution was excluded in meta-heuristic. For
606 instance, revenue from fertilizer sale is obvious regardless of solution quality. For the sake of

607 simplicity, these factors were not included in the SA algorithm. Instead, they were appended at
608 the end of the algorithm to display the total net present value. Thus, the objective function
609 formula was shortened. The objective function was formulated in Equation 23 as given follows:

$$\begin{aligned} 610 \text{ Max (NPV)} &= D(i,n) \times (\text{HHES} + \text{CHES} - \text{RMTC} - \text{HHETC} - \text{CHETC} - \text{PPOMC} - \text{PLNOMC} - \\ 611 &\text{ETLLC}) - \text{PPTIC} - \text{PLNTIC} - \text{ETTIC} \end{aligned} \quad (23)$$

612 Where HHES, CHES, RMTC, HHETC, CHETC, PPOMC, PLNOMC, ETLLC, PPTIC,
613 PLNTIC, ETTIC represent hot heat energy sale, cold heat energy sale, raw material
614 transportation cost, represent hot heat energy-transportation cost, cold heat energy-transportation
615 cost, operation & maintenance costs of power plant and pipeline network, electricity
616 transmission line loss cost, power plant, pipeline network, and electricity transmission total
617 installation cost, respectively.

618 Before the construction of the algorithm, the neighborhood search strategy, which is the crucial
619 part of a SA algorithm, was determined. The proposed algorithm selects a neighbor solution by
620 generating a random integer number, which has a uniform distribution between 1 and 127. Each
621 number represents a candidate power plant location. If there is a power plant at the location of
622 the generated number, the power plant is not installed and its value (1) is switched to 0 and
623 vice versa.

624 After determining neighbor search strategies, two solution approaches were developed. In the
625 first approach, the entire search space was explored to understand the trajectory of the solution
626 based on the number of power plants. There is no constraint associated with a number of the
627 power plant in this algorithm. All of the 127 power plants can be established. In this algorithm,
628 initial temperature and final temperature were calculated based on the best and the worst
629 solution. The algorithm intends to most likely establish one power plant to maximize net present
630 value. This makes sense since the fact that fixed establishment costs such as power plant
631 installation cost; power line installation cost and transformer cost are rather high. These costs can
632 reach up to 6 million euros for every power plant. The other reason for such a trend of the
633 algorithm is the lowness of raw material transportation cost. Those two factors mainly influence
634 the algorithm trajectory.

635 Control parameters were adjusted for the first case. P_i and P_f were taken as 0.96 and 0.01,
636 respectively. The number of moves for each temperature was taken as sufficiently large value to
637 search the entire space. In the first SA algorithm, it was taken as 1000.

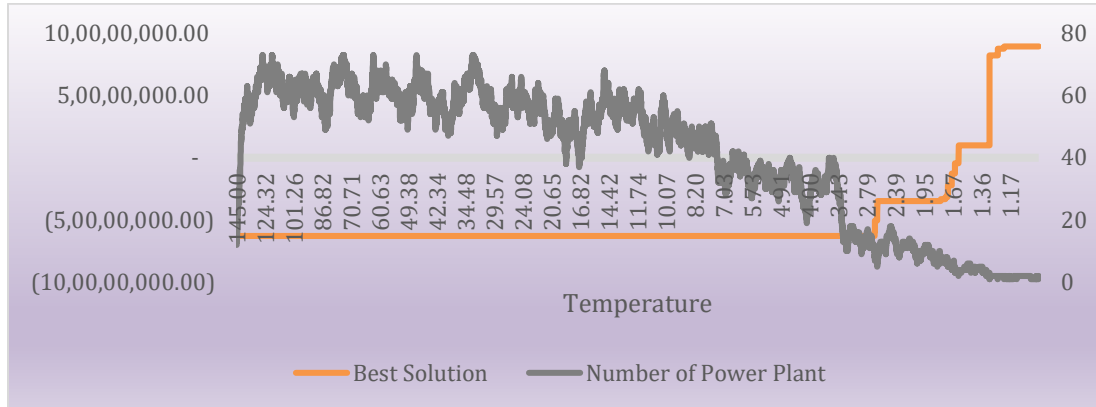
638 The control parameters of the first approach were presented as follows.

639 $T_0 = 145$, It was calculated based on the Eq. 21.

640 $T_f = 1$, It was calculated based on the Eq. 21.

641 $a = 0.95$, It was predetermined.

642



643

644 Figure 5. Treatment of the SA algorithm based on the first approach

645

646 Just one power plant was installed at the point where net present value peaks based on the result.

647 This reveals that establishing more than one power plant restrain finding a better solution. It was

648 decided that one power plant establishment most likely seems to an optimum solution. Then, the

649 second algorithm, which narrows the solution space, was developed. In this algorithm, one

650 power plant was set in the initial solution and a power plant was selected randomly as a

651 neighborhood search. The probability of selecting each power plant has a uniform distribution. If

652 the selected power plant is set already as 1, then it was set as 0 and vice versa. Thus, it was

653 allowed that just one power plant could be established. In the second approach, T_0 and T_f were

654 recalculated since the minimum value of fitness function was changed. In this algorithm, the

655 number of moves (N) was taken 127, which equals to the number of variables (power plant).

656 Control parameters which were used in the second algorithm were demonstrated as; $T_0 = 224$; T_f

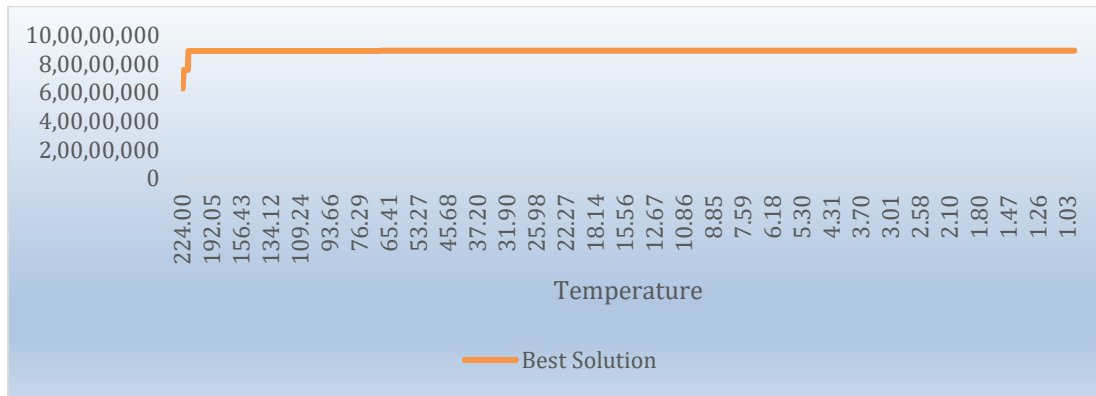
657 $= 1$; $a = 0.95$; $N = 127$; $P_i = 0.96$; $P_f = 0.01$.

658 The proposed algorithm was run on an Intel Core Quad 2.4 GHz CPU with 8 Gb Ram on a 64-bit

659 platform a few times and the best solution was found in every execution. The computational time

660 took almost 180 seconds on average. The iterative treatment of the algorithm was demonstrated

661 in Figure 5-6 as given follows;



662

663

Fig 6. Treatment of the SA algorithm based on the second approach

664 Based on the result, the second algorithm got the same result just as the first algorithm.

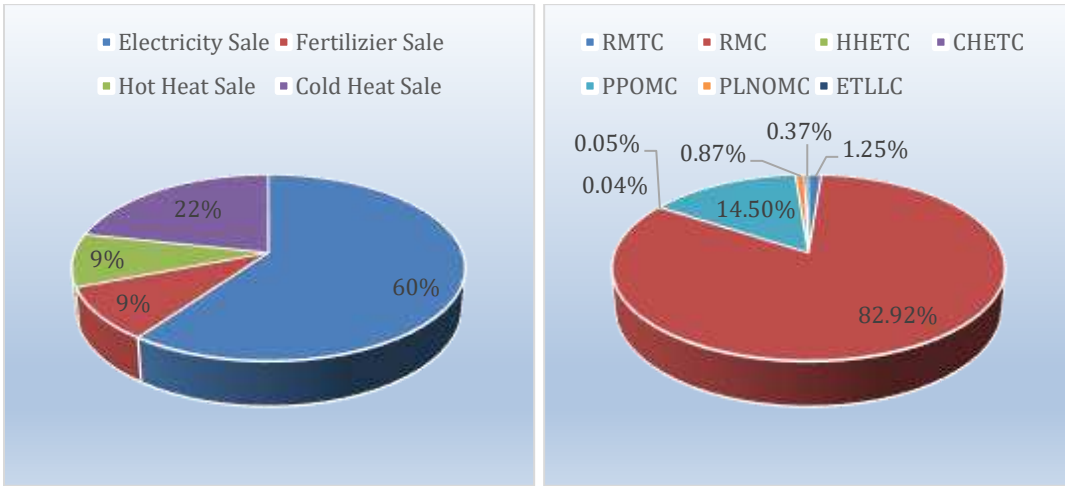
665 Narrowing the search space reduced the computational time by nearly 90%.

666 4. The results and discussion

667

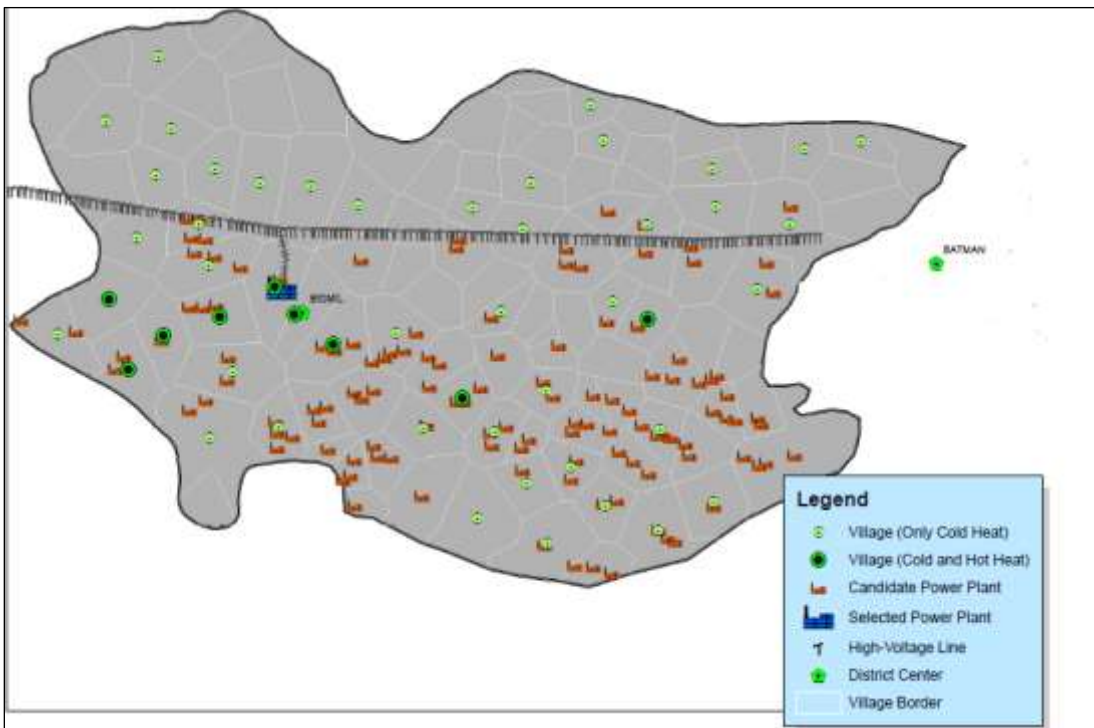
668 Based on the results of the SA model, just one power plant with an installed power of 29,09 MW
 669 has been established. It can be concluded that high installation cost a power plant and the low
 670 unit cost of raw material transportation has a strong impact on the establishment of just one
 671 power plant. 0.15 % of the electricity produced is lost due to the distance between the power
 672 plant and the nearest connection point. The nine settlements for which the hot heat energy was
 673 supplied also received the cold heat energy. The eight settlements receive their whole hot heat
 674 demand, while 1 settlement receives 5 % of its hot heat demand. 41 settlements receive only cold
 675 heat energy. The reason behind the fact that more settlements received cold heat energy is
 676 relatively high price and low demand for cold heat energy compared to hot heat energy. All
 677 settlements completely received their cold heat demand. The amount of heat produced is highly
 678 greater than the total cold heat demand of all settlements even if losses are considered.

679 99.33 % of the produced hot heat was sold to settlements, however, 80.43 % of the hot heat
 680 demand was met. 66.86 % of the cold heat was sold to settlement and cold heat demand was met
 681 completely. 0,67 % of the hot heat, 1.3 % of the cold heat and 0.37% of the electricity were lost
 682 while transferring. On the other hand, proportional distributions of income and expenses through
 683 project lifetime were illustrated in Figure 7 as follows. As might be seen from the figure,
 684 electricity sales in revenue items and power plant establishment cost in expenditure items are by
 685 far the most effective factors than others.



686
687 Figure 7. The revenues by product and expenditures by operations (SA Algorithm)
688

689 The share of raw material transportation cost (RMTIC) is relatively low as might be observed
690 from Figure 8. This resulted from quite a low cost of unit transportation cost of raw material and
691 the short distance between parcels and power plants. Besides, electricity transmission line cost
692 (ETLLC), hot and cold heat transferring cost (HHETC and CHETC) are relatively low since
693 proposed power plant locates very close to the city center, where demands the major portion of
694 the total heat, and power line, respectively (see Figure 8).



695

696

Figure 8. Final depiction of the problem

697 **5. Conclusion**

698
699 In this study, a GIS based simulated annealing algorithm has been proposed and applied to a
700 real-world problem (Bismil District in Diyarbakır, Turkey). The results are promising in terms of
701 the performance of the SA algorithm and attractive for a potential investment. Large-scale
702 combinatorial problems related to bioenergy supply chain problems can be solved by utilizing
703 the proposed SA heuristic. The treatment of the proposed algorithm was observed in an extensive
704 search space. The algorithm was run many times with a different set of control parameters to
705 exactly understand solution trajectory. The experiments showed that the installation of one
706 power plant is the optimum.

707 This study is the first in terms of utilizing simulated annealing in a trigeneration system, which is
708 designed for the biomass-to-bioenergy supply chain. For future studies, assumptions of this
709 model can be improved. and in this way, a real-world problem can be dealt with more
710 realistically. In addition to assumptions, control parameters of the proposed SA algorithm could
711 be adjusted based on different strategies. Besides, a population-based algorithm can be utilized in
712 the bioenergy supply chain in cases wherein trade-offs are very decisive.

713
714 Financial support for this work was provided by the Gaziantep University, Department of
715 Scientific Research Projects. This support is gratefully acknowledged. Grant number:
716 MF.YLT.17.14.

717 **References**

718 IEA-International Energy Agency-. (2017). *Technology Roadmap Delivering Sustainable*
719 *Bioenergy*. Paris: International Energy Agency.

720 Akgül, A., Seçkiner, S.U. (2019). Optimization of biomass to bioenergy supply chain with tri-
721 generation and district heating and cooling network systems. *Computers & Industrial*
722 *Engineering*. 137, 106017.

723 Toklu, E., (2017), Biomass energy potential and utilization in Turkey, *Renewable Energy*, 107,
724 235-244.

725 General Directorate of Energy Affairs. (2018). *Renewable Energy*. Retrieved April 2019, from
726 <http://www.yegm.gov.tr/anasayfa.aspx>

727 Kumar, A., Sokhansanj, S., & Flynn, P. C. (2006). Development of a multi-criteria assessment
728 model for ranking biomass feedstock collection and transportation. *Applied Biochemistry and*
729 *Biotechnology* , 129, 71-87.

730 Turkenburg, W.C. (2000). Renewable energy technologies. In J. Goldemberg (Ed.), *World*
731 *energy assessment: Energy and the challenge of sustainability* (pp. 219-273). NY, USA.

732 Ciria, P., & Barro, R. (2016). *Biomass Supply Chains for Bioenergy and Biorefining/Biomass*
733 *resource assessment* (1 ed.). Woodhead Publishing.

734 Yue, D., & You, F. (2016). Biomass and biofuel supply chain modeling and optimization. In
735 *Biomass Supply Chains for Bioenergy and Biorefining* (pp. 149-166). Evanston, IL, United
736 States: Woodhead Publishing.

737 Ghaderi, H., Pishvae, M., & Moini, A. (2016). Biomass supply chain network design: An
738 optimization-oriented review and analysis. *Industrial Crops and Products* , 94, 972-1000.

739 Celli, G., Ghiani, E., Loddo, M., Pilo, F., & Pani, S. (2008). Optimal location of biogas and
740 biomass generation plants. *International Universities Power Engineering Conference*. Padova,
741 Italy.

742 Sultana, A., & Kumar, A. (2012). Optimal siting and size of biorefinery facilities using
743 geographic information system. *Applied Energy* , 94, 192-201.

744 Rache-Lopez, P., Ruiz-Reyez, N., Galan, S. G., & Jurado, F. (2009). Comparison of meta-
745 heuristic techniques to determine optimal placement of biomass power plants. *Energy*
746 *Conversion and Management* , 50, 2020-2028.

747 Rentizelas, A., Tatsiopolous, I., & Tolis, A. I. (2009). An optimization model for multi-biomass
748 tri-generation energy supply,. *Biomass and Bioenergy* , 33 (2), 223-233.

749 Vera, D., Carabias, J., Jurado, F., & Ruiz-Reyez, N. (2010). A Honey Bee Foraging approach for
750 optimal location of a biomass power plant. *Applied Energy* , 87, 2119–2127.

751 Goodchild, M. F. (1997). *What is geographic information science?* Santa Barbara, USA.

752 Alibaş, İ., Özsoy, G., & Eliçin, K. (2015). Diyarbakır İl Tarımsal Kaynaklı Biyogaz
753 Potansiyelinin Belirlenmesi. *Tarım Makineleri Bilimi Dergisi* , 11, 75-87.

754 Kirkpatrick, S., Gelatt, D., & Vecchi, M. P. (1983). Optimization by Simulated Annealing.
755 *Science*, 220 (4598), 671-680.

756 Metropolis, N., Rosenbluth, A. W., Rosenbluth, M. N., Teller, A. H., & Teller, E. (1953).
757 Equation of state calculations by fast computing machines. *The Journal of Chemical Physics* ,
758 21, 1082-1091.

759 Castillo-Villar, K. K. (2014). Meta-heuristic Algorithms Applied to Bioenergy Supply Chain
760 Problems: Theory, Review, Challenges, and Future. *Energies* , 7, 7640-7672.

761 Seçkiner S.U. (2005). Implicit and heuristic solution approaches for workload balanced tour
762 scheduling problems. Gazi University. *PhD Thesis*.

763

764

765

766

767

768

769

770

771

772

773

774

775

776